(20) Dubault, A.; Deloche, B.; Herz, J. *Macromolecules* **1987**, *20*, 2096.
(21) Lifshits, M. I. *Polymer* **1987**, *28*, 454.
(22) Abraghams, A. *The Principles of Nuclear Magnetism*; Oxford University Press: New York, 1961.
(23) Slichter, C. P. *Principles of Magnetic Resonance*; Springer-Verlag: Berlin, 1978.
(24) Kubo, R. In *Fluctuation, Relaxation and Resonance in Magnetic Systems*; ter Haar, D., Ed.; Oliver & Boyd: Edinburgh, U.K., 1962.
(25) Mc Call, D.; Douglass, D.; Anderson, E. *J. Polym. Sci.* **1962**, *59*, 301.
(26) Heatley, F. In *Static & Dynamic Properties of the Polymeric Solid State*; Pethrick, R. A., Richards, R. W., Eds.; Riedel: Dordrecht, The Netherlands, 1982.
(27) Ullman, R. *J. Chem. Phys.* **1965**, *43*, 3161.
(28) Wright, P. Thesis, University of Leeds, 1988.
(29) Brereton, M. G. *Macromolecules*, in press.
(30) Anderson, P. W.; Tomita, K. *Rev. Mod. Phys.* **1953**, *25*, 269.
(31) Mc Connell, J. *Polymer* **1985**, *26*, 193.
(32) de Gennes, P.-G. *Scaling Concepts in Polymer Physics*; Cornell University Press: Ithaca, NY, 1979.
(33) Brereton, M. G.; Williams, T. *J. Phys. A* **1985**, *18*, 2033.
(34) Cohen-Addad, J. P. *J. Phys.* **1982**, *43*, 1509.
(35) Rouse, P. *J. Chem. Phys.* **1953**, *21*, 1272.
(36) Doi, M.; Edwards, S. F. *The Theory of Polymer Dynamics*; Clarendon Press: Oxford, 1986.
(37) Warner, M. *J. Phys. C* **1981**, *14*, 4985.
(38) Flory, P. J. *Macromolecules* **1979**, *12*, 119.
(39) Edwards, S. F.; Deam, R. T. *Philos. Trans. R. Soc. London A* **1976**, *280*, 317.
(40) Cohen-Addad, J. P.; Schmit, C. *Macromolecules* **1989**, *22*, 142.

Static and Dynamic Properties of Poly(ethylene oxide) in Methanol

Pu Zhou and Wyn Brown*

Institute of Physical Chemistry, University of Uppsala, Box 532, 751 21 Uppsala, Sweden.
Received April 27, 1989; Revised Manuscript Received July 18, 1989

ABSTRACT: The properties of poly(ethylene oxide) PEO chains in dilute and semidilute solutions in methanol have been examined using pulsed-field-gradient NMR and static and quasielastic light scattering (QELS). From the temperature dependence of the second viral coefficient the Θ temperature was determined to be close to 16.7 °C. Values of the inverse osmotic compressibility ($\partial\pi/\partial C$), determined independently from static LS and the ratio of the respective diffusion coefficients (D_{QELS}/D_{NMR}) in dilute solution, were identical within experimental uncertainty and are precisely described by renormalization group theory. The latter also provides a good fit for the concentration dependence of the diffusion coefficient. The self-diffusion coefficients are represented by a universal curve: log (D/D_0) versus log (C/C^*). The dynamic light-scattering measurements showed the presence of molecular clusters (or ordered domains), which appear to constitute a general feature of PEO solutions in both good and poor solvent quality. These clusters diminish in size as the temperature is raised and/or the concentration is lowered. Data for hard spheres (stearic acid coated SiO_2) diffusing in the PEO solutions formed a universal curve, log (D/D_0) versus log (C/C^*), independent of sphere size and gave a dependence on matrix MW of $M^{-0.58}$. Clusters of size similar to the hard spheres have an apparent diffusion rate that is 1 order of magnitude slower at the same matrix polymer concentration.

Introduction

Poly(ethylene oxide) (PEO) has attracted considerable interest for its unusual properties; it is soluble not only in water but also, for example, in dioxane, chloroform, methanol, and benzene. There is also a pronounced tendency for PEO to associate in solution: this has been demonstrated by light-scattering measurements, even in very dilute aqueous solutions,[1-7] and short chains may form spherulites.[3] It would appear, however, that these aggregates, reflected in a slow mode in dynamic light scattering in water solution, represent only a small weight fraction of the material in the solution. Thus, classical gradient diffusion on the high molecular weight polymer gives D values that agree almost precisely with the fast mode deriving from the molecularly dispersed polymer.[6]

In light of the ambiguities, which may have resulted from aggregation in aqueous solutions and which place in question some of the conclusions drawn in earlier studies, it seemed worthwhile to reexamine the behavior of this important polymer in a more congenial solvent. Methanol appears to be such a solvent. Moreover, the Θ state is accessible in methanol in the vicinity of 17 °C, which allows one to examine the influence of solvent quality by varying the temperature. In addition, PEO has a unique proton signal making it possible to perform pulsed-field-gradient NMR (PFG-NMR) measurements of self-diffusion on PEO in the solutions. For this reason, deuteriated methanol (CD_3OD) has been employed as the solvent. This is convenient since, through combination of dynamic light-scattering (QELS) and NMR diffusion coefficients, one may evaluate the thermodynamic contribution to the former quantity in dilute solution and in turn test various theoretical predictions.

Experimental Section

Poly(ethylene oxide) samples were narrow distribution fractions obtained from Toya Soda Ltd., Tokyo. The molecular weights, polydispersities, etc., are provided by the manufacturer.

designation	$M \times 10^{-3}$	M_w/M_n
SE-5	40	1.03
SE-8	74	1.02
SE-15	145	1.04
SE-70	594	1.10
SE-150	1200	1.12

0024-9297/90/2223-1131$02.50/0

Table I
Dilute Solution Properties of PEO in Methanol (25 °C)

$M \times 10^{-3}$	R_g, Å	$A_2 \times 10^4$, mol mL g^{-2}	$D^*_0 \times 10^{11}$, $m^2\ s^{-1}$	$M/RT(\partial\pi/\partial C)$ (C = 0.5%)	θ, °C	$[\eta]^a$, mL g^{-1}	C^*, %	C_E, %
40	83[b]	29.5	8.23	2.18	16.1	37	2.7	4.9
74	120[b]	28.3	5.92	3.14	17.2	53	1.9	2.6
145	182	23.9	4.05	4.48	16.7	78	1.3	1.3
594	410	18.7	1.63	11.15	17.0	177	0.56	0.33
1200	620	17.6	1.10	17.2	16.5	265	0.4	0.16

[a] $[\eta] = 79.5 \times 10^{-3} M^{0.58}$. [b] Calculated from $R_g = 0.16M^{0.585}$.

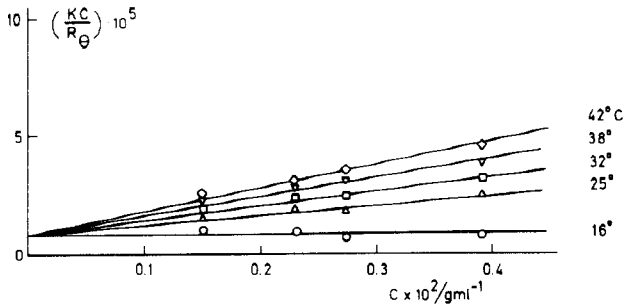

Figure 1. Intensity light-scattering data on the PEO (M = 1.45×10^5)/methanol system: KC/R_θ versus C at different temperatures.

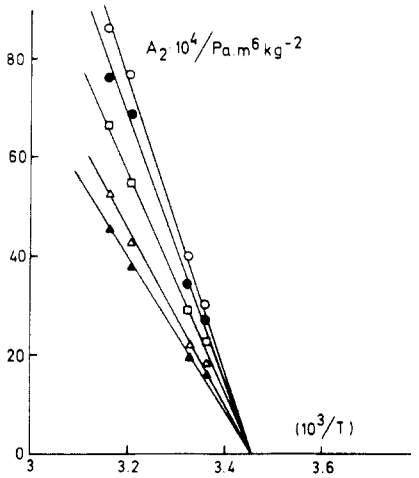

Figure 2. Estimation of the θ temperature in the PEO/methanol system. Molecular weights: 4×10^4 (○); 7.4×10^4 (●); 1.45×10^5 (□); 5.94×10^5 (△); 1.2×10^6 (▲).

Sterically stabilized silica particles were kindly provided by Professor A. Vrij, Utrecht, The Netherlands, and are the materials employed in ref 38. The radii were 1595 and 280 Å.

Deuteriated methanol was obtained from Merck, FRG, and used for the PFG-NMR measurements (see below).

Pulsed-field-gradient NMR measurements were made as described previously.[1,22]

Static Light Scattering. Intensity light-scattering measurements were made using a photon-counting apparatus supplied by Hamamatsu to register the scattered signal. The light source was a 3-mW He–Ne laser. The optical constant for vertically polarized light is $K = 4\pi n_0^2(dn/dc)^2/N_A\lambda^4$, where n_0 is the solvent refractive index, dn/dc the measured refractive index increment (=0.134 mL g^{-1} at 25 °C), and λ the wavelength (633 nm). The reduced scattered intensity, KC/R_θ, was derived where C is the concentration and R_θ is the Rayleigh ratio obtained through calibration using benzene; $R_{90} = 8.51 \times 10^{-6}$.[48] The angle-corrected intensity for benzene was constant over the angular range 45–135°. Precise measurements of the angular dependence of KC/R_θ could be made for the three fractions with $M > 1.48 \times 10^5$ and gave the radius of gyration, R_g: see Table I. The inverse osmotic compressibility was evaluated from the KC/R_θ values; see eq 2 below.

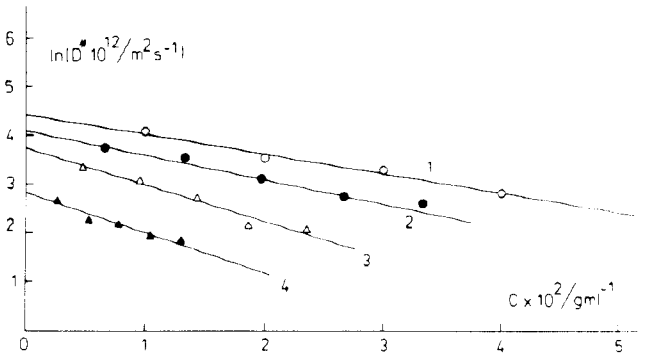

Figure 3. Pulsed-field-gradient NMR data showing self-diffusion coefficients (D^*) as a function of concentration for the fractions with MW: (1) 4×10^4; (2) 7.4×10^4; (3) 1.45×10^5; (4) 5.94×10^5.

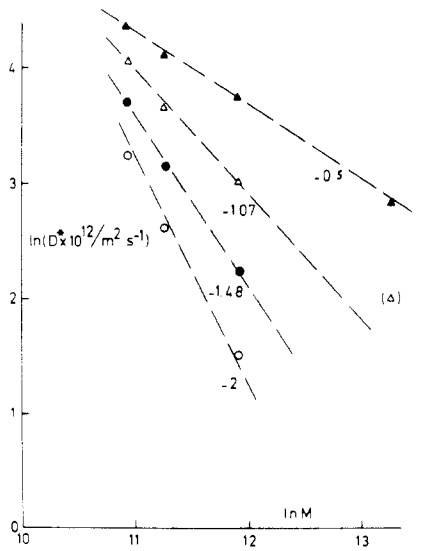

Figure 4. Molecular weight dependence of the self-diffusion coefficients in the PEO/methanol system. C = 0 (▲); 1% (△); 2% (●); 3% (○). Slopes are shown inserted.

Dynamic light-scattering measurements (in CH_3OH) have been made using the apparatus and technique described in ref 12. Laplace transformation of the correlation curves was performed using a constrained regularization program REPES[15] to obtain the distribution of decay times. The algorithm differs in a major respect from CONTIN[16] in that the program directly minimizes the sum of the squared differences between the experimental and calculated $g^2(t)$ functions using nonlinear programming, and the a priori chosen parameter "probability to reject" was selected as P = 0.5. The decay time distributions were similar to those obtained using CONTIN with a similar degree of smoothing.

Intrinsic viscosity measurements were made at 25 °C using an Ubbelohde capillary viscometer.

Results and Discussion

Static light-scattering results are summarized in Table I. For the samples having molecular weights greater than

10^5, it was possible to determine the radii of gyration from the average slopes of plots of KC/R_θ at angles greater than 60°. At low angles there is a significant downturn in KC/R_θ due to the presence of larger particles (see below). Approximate values of R_g for the lower molecular weights were estimated using the relationship $R_g = 0.16M_w^{0.585}$, which applied to the higher molecular weights.

The MW dependence of A_2 is given by $A_2 \sim M^{-0.2}$.

Static light-scattering measurements were also made as a function of temperature over the range 16–42 °C in order to determine the Θ temperature for the PEO/methanol system. Such data are illustrated in Figure 1 for the fraction having $M = 1.45 \times 10^5$, and they show that the Θ temperature lies in the vicinity of 17 °C. By plotting the data as shown in Figure 2 in a diagram of A_2 versus T^{-1}, where T is the absolute temperature, an average value of Θ = 16.7 °C was found for the different fractions independent of MW.

Pulsed-field-gradient NMR measurements on PEO fractions in CD_3OD gave values of the self-diffusion coefficient (D^*). Data at 25 °C are summarized in Figure 3. Measurements on the fraction with $M = 1.2 \times 10^6$ could not be made at this temperature due to the weak signal. However, it was possible to make the NMR determinations with acceptable precision at 45 °C, and the self-diffusion coefficients were then corrected to 25 °C using the relationship

$$D^*_{25} = D^*_{45}(\eta_{45}/\eta_{25})(298/313) \quad (1)$$

Values of D^* at infinite dilution (D^*_0) were estimated by extrapolation of the linear plots in Figure 3 and are included in Table I. The molecular weight dependence of D^* at infinite dilution and several concentrations is illustrated in Figure 4. When the C^* values in Table I (with $C^* \approx 1/[\eta]$) are used, , all samples are in the semidilute range above $C = 3\%$. The MW dependence of D^* increases with increasing concentration from a slope of about −0.5 at $C = 0$, representing Zimm behavior, to a slope of −2 at about $C = 3\%$, which is the anticipated slope for systems at semidilute concentrations according to scaling theory:[47] $D^* \sim M^{-2}C^{-1.75}$ (good solvent) and $D^* \sim M^{-2}C^{-3}$ (Θ solvent). The change in the MW dependence with concentration may derive either from crossover behavior or, alternatively, from a progressive increase in the congestion of the system (see below). Kim et al.,[9] however, observed a smooth increase in the molecular weight dependence up to a value of M^{-3}. This is similar to the trend reported for the polystyrene/poly(vinyl methyl ether) ternary system by Wheeler et al.[10] They found that the exponent increased from −0.55 to +1.89 at the highest concentration (0.1 g mL^{-1}). As interpreted by Nemoto et al.,[11] the deviation of D^* from $D^* \sim M^{-1}$ (which is the Zimm exponent when hydrodynamic screening is fully taken into account) reflects the influence of topological interactions between the labeled chain and those surrounding it.

Figure 5 shows the concentration dependence of the self-diffusion coefficients in a double-logarithmic diagram of the reduced diffusion coefficient versus the reduced concentration, C/C^*. It was shown previously[12] for data in the homopolymeric polyisobutylene system (PIB_1/PIB_2/chloroform) that self-diffusion data are well represented in such a universal curve. The data approximate a smooth curve as has been demonstrated by other workers using PFG-NMR[9,13] and forced Rayleigh scattering (FRS).[14] When the results are compared with the predictions of theory, the usual interpretation has been that in good solvents the tangent over a limited range of

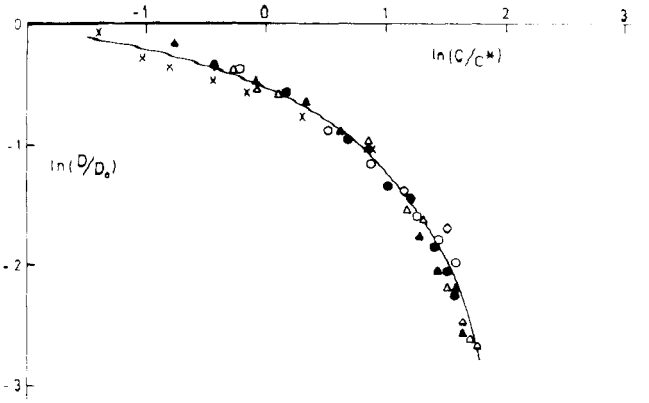

Figure 5. Comparison of self-diffusion coefficients for PEO fractions (NMR data) with those for the SiO_2 hard spheres (R_H = 1595 Å) in PEO of $M = 5.94 \times 10^5$ (DLS data at $\theta = 20°$). Molecular weights of PEO: 4×10^4 (○); 7.4×10^4 (●); 1.45×10^5 (△); 5.94×10^5 (▲). log–log plot of the reduced diffusion coefficient (D/D_0) versus the reduced concentration (C/C^*) where $C^* = 1/[\eta]$. Data for SiO_2 spheres (×).

concentration is consistent with the expected slope of −1.75. A tangent of −3 at higher concentrations has been taken to indicate coil contraction to Θ dimensions in the increasingly congested system as the solvent becomes poorer. In this way the present data cannot refute a slope of −3 at the highest concentrations. However, such a conclusion can at best demonstrate that the experimental data are not inconsistent with the predictions of reptation since with the observed curvature this conclusion may be trivial. When the concentration range is extended in order to try and prove the point, monomer–monomer friction effects must also be corrected for[13] creating an additional source of ambiguity. It is important to note that the slow mode revealed in the DLS measurements (below) has a similar dependence on concentration although, at a given value of C, D_{slow} is about 1 order of magnitude slower than D^* and thus cannot be attributed to self-diffusion of the single chain. A recent communication[12] established that hard spheres follow the same D/D_0 versus C/C^* curve, an observation that provides strong evidence that reptation is not the relevant mechanism. Data are thus included in this plot for the large SiO_2 spheres (Figure 16) in a matrix of PEO (5.94×10^5) and serve to indicate the common mechanism for diffusion in congested systems.

Figure 6 shows the relationship between the bulk viscosity and the reduced concentration, C/C^*. It is seen that a universal curve is again obtained for the various molecular weights with a slope of 3.6 in the higher concentration range.

Dynamic Light Scattering. The correlation functions are always bimodal as shown by typical decay time spectra in Figure 7. These spectra have been obtained using the REPES program,[15] which is a modified form of CONTIN[16] allowing rapid Laplace inversion on data of wide time scales. This procedure is described in more detail in the section on treatment of data. Both main components are formally diffusive as shown by the relationship between the relaxation rate (Γ) and q^2 in Figure 8, where q is the scattering vector ($q = (4\pi n/\lambda)[\sin(\theta/2)]$).

Figure 9a shows the two modes as a function of concentration for three molecular weights while Figure 9b shows how the relative intensity of the slow mode increases with increasing concentration; see below. With increasing concentration, the relaxation rate of the fast mode increases while that for the slow mode decreases strongly. It may be noted that, at a given concentration,

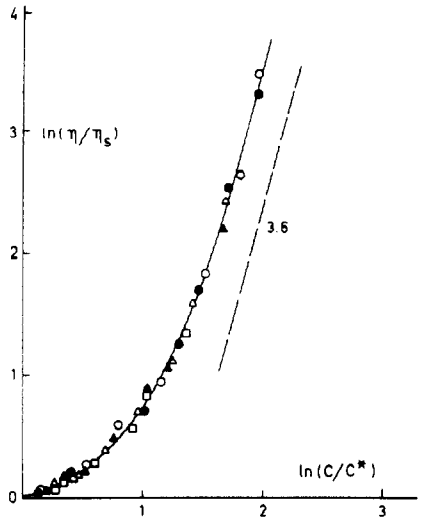

Figure 6. log–log plot of the bulk solution viscosity (η) reduced by the solvent value versus the reduced concentration (C/C^*) ($M = 4 \times 10^4$ (○); 7.4×10^4 (●); 1.45×10^5 (□); 5.94×10^5 (△); 1.2×10^6 (▲)).

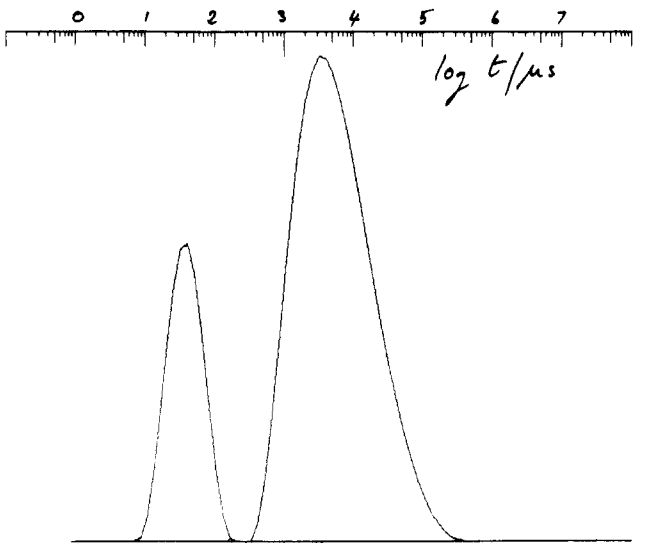

Figure 7. Decay time distributions in the system: PEO ($M = 5.94 \times 10^5$) in methanol at 35 °C, $C = 1.31\%$, and a measurement angle of 120°. The fast mode corresponds to the "blob" diffusion and the slow to the translation of clusters of chains. The quantity $\tau A(\tau)$ is plotted on the ordinate to give an equal area representation.

the slow mode is characterized by a decay time much longer (at least 1 order of magnitude) than that corresponding to self-diffusion determined by PFG-NMR (see Figure 11). With the fast mode there is a clear change in slope at C^* in the latter figure. Above C^* the slope is 1.0, after correction for backflow.[17] The slow mode has a slope of −2.5. Since the MW dependence (taken at the point marked by the broken line in Figure 9a) is also about −2, it is easy to understand why the slow mode observed in light-scattering experiments has earlier been confused with the single-chain self-diffusion coefficient.[18-20] As stressed before,[38] this value for the MW exponent also characterizes diffusion in congested systems and is not in itself a sufficient signature for reptation. Skolnick et al.[21] have established this point by Monte Carlo simulations. We note also the progressive increase of the MW dependence of the self-diffusion coefficient with concentration shown in Figure 4. As concluded from similar data in the PEO/water system,[4] water being a thermodynamically good solvent, the slow mode probably arises from the presence of molecular clusters, which apparently occur with PEO in most solvents, and thus is not related to the closeness to the Θ point. We have also noted similar decay time spectra in chloroform and dioxane, which are also relatively good solvents for PEO.[2] Clusters (or ordered domains) are not peculiar to PEO but apparently are a feature of both aqueous systems, e.g., poly(vinylpyrrolidone)[50] and poly(methacrylic acid)[51] in water, and nonaqueous systems, e.g., polystyrene in ethyl acetate.[52]

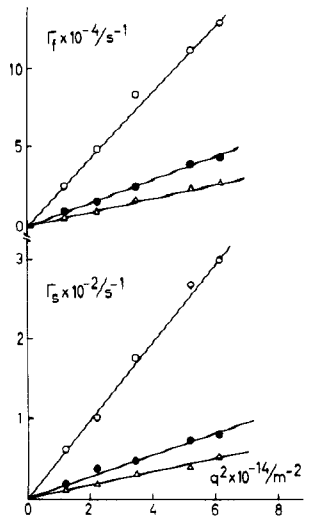

Figure 8. Relaxation rates (Γ) for the fast and slow modes (cf. Figure 7) as a function of the scattering vector, q ($M = 1.45 \times 10^5$ (○); 5.94×10^5 (●); 1.2×10^6 (△).

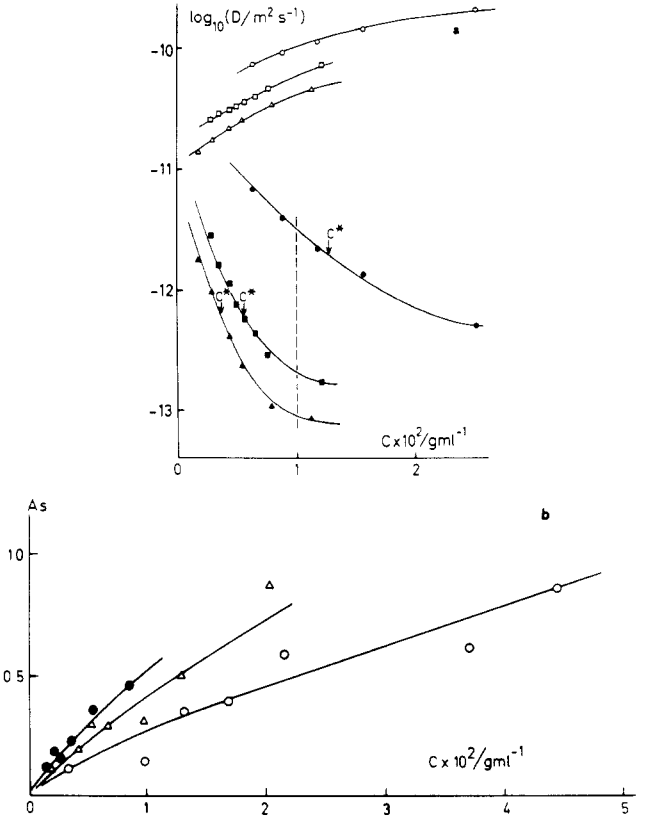

Figure 9. (a) Concentration dependences of the fast and slow modes for the molecular weights: $M = 1.45 \times 10^5$ (circles); 5.94×10^5 (squares); 1.2×10^6 (triangles). The molecular weight dependence for the slow mode at the vertical dotted line is −2. (b) Relative amplitudes of the slow mode as a function of concentration for three molecular weights: 4×10^4 (○); 1.45×10^5 (△); 1.2×10^6 (●).

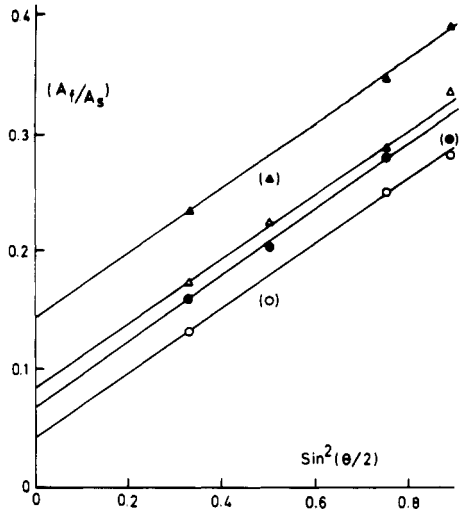

Figure 10. Plots of the amplitude ratio (A_f/A_s) versus $\sin^2(\theta/2)$ for the QELS data on $M = 5.94 \times 10^5$ at different temperatures. From the slopes it is possible to make approximate estimates of the apparent size of the clusters giving rise to the slow mode. Temperatures: 25 (○); 35 (●); 45 (△); 55 °C (▲).

The two diffusive modes are observable in the dynamic light-scattering experiment as a consequence of the size polydispersity in the system. As shown by Phillies[23] and Pusey et al.[24] for hard spheres and Benmouna et al.[25] for linear chains, the signal from one species will be modulated by the second, leading to a bimodal autocorrelation function. The two relaxation rates correspond to the collective diffusion coefficient (D_c) on the one hand and the interdiffusion coefficient (D_I) on the other. At a suitably low concentration of the minor component, one obtains the self-diffusion coefficient. Recent work[12] has demonstrated that accurate measurements of the self-diffusion coefficient may be determined in this way in homopolymeric mixtures of two molecular weights. It is concluded that in the present case the slow mode derives from the apparent mobility of molecular clusters or ordered domains. It should be noted that the presence of clusters does not significantly influence the PFG-NMR self-diffusion coefficients in contrast to the QELS measurements. This is because in a polydisperse system the former measurements essentially yield the number-average quantity[49] whereas the diffusion coefficient from QELS is a z-average.

In order to assess the size and stability of the latter, measurements were made as a function of temperature over the range 25–55 °C. Plots were made of the ratio of the relative intensities of fast and slow modes, A_f/A_s, versus $\sin^2(\theta/2)$ at each temperature. Assuming that the fast mode, representing the collective motions of the chains in semidilute solution, is angle-independent when $qR_g \ll 1$, as is well-known to be the case in semidilute non-Θ-state solutions, all observed dependence on $\sin^2(\theta/2)$ should derive from the slow diffusive component. This approach was first used by Sedlak et al.[51] Figure 10 shows such plots obtained using the fraction with $M = 5.94 \times 10^5$ at a concentration of 1.3%. The average size of the clusters decreases significantly with increasing temperature from about 1730 Å at 25 °C to 930 Å at 55 °C. These estimates of the apparent radii are only approximate, owing to the uncertainty in the relative amplitudes. At a given angle, the relative amplitude does not change greatly with change in temperature, meaning that the weight fraction of clusters does not decrease substantially although their average size does. Similar estimates were made as a function of concentration. The clusters decreased in average size from 1730 Å at 1.3% to 960 Å at 0.37%.

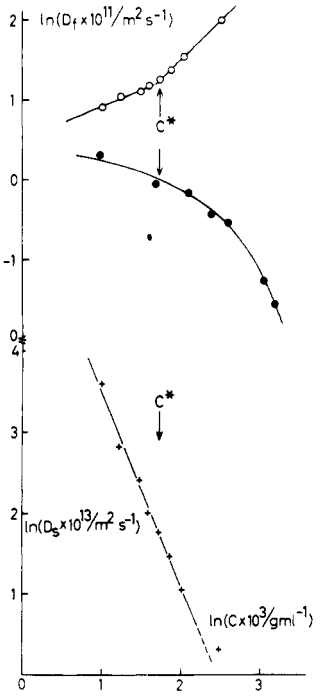

Figure 11. log–log plots of D versus C for QELS data (PEO, 5.94×10^5) (fast (○) and slow (+) modes) compared with the self-diffusion coefficients for single chains from NMR measurements (●). Above C^* the slope for the fast mode is about unity and for the slow mode −2.5.

The number and/or size of the clusters increases, however, with decreasing molecular weight, possibly owing to facilitated packing for short, more extended, chains. Burchard and Polik[3] examined PEO in aqueous solution and have suggested that for molecular weights below about 20 000 spherulites are formed. The slow component may, however, derive from only a small part of the total polymer present. As was shown[6] from gradient diffusion measurements, the average diffusion coefficient was found to be identical with the fast mode determined in light-scattering measurements.

The inverse osmotic compressibility, $(\partial\pi/\partial C)_{T,P}$, provides the response in the system to relax the concentration fluctuations in a polymer solution. Experimentally, one may determine $(\partial\pi/\partial C)$ with good precision from static light-scattering measurements employing the scattered intensity extrapolated to zero angle:

$$(KC/R_\theta) = [M_w/RT](\partial\pi/\partial C)_{T,P} = (1 + 2A_2CM_w + ...) \quad (2)$$

This quantity may also be obtained from the measured dynamic quantities D_{QELS} and D_{NMR} since the former is also related to the right-hand side of eq 2. Here we employ the fast mode, D_f, from QELS since it represents single-chain properties in dilute solution and the cooperative motions of the network above C^*. Thus

$$D_{QELS}/D_{NMR} = [M/RT](\partial\pi/\partial C)_{T,P} \quad (3)$$

The assumption is implicit here that the frictional coefficients determined by QELS and by self-diffusion measurements are identical, whereas it is known that $f_{QELS} > f_{NMR}$.[26,27] However, at dilute concentrations we show in Figure 12a below that the ratio between the dynamic quantities is $D_{QELS}/D_{NMR} = KC/R_\theta$, within experimental uncertainty for three molecular weights, and that the

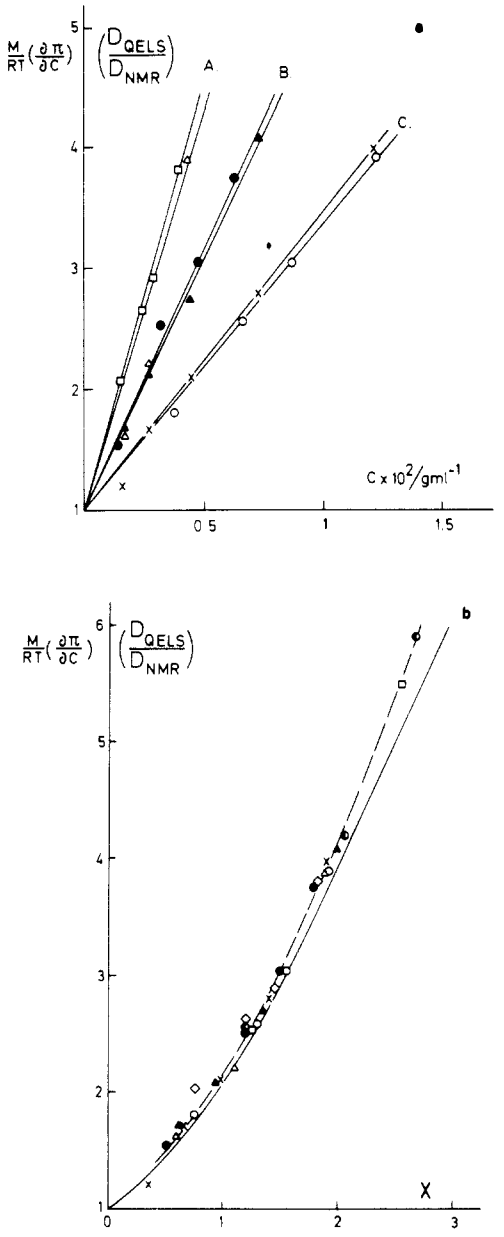

Figure 12. (a) Comparison of osmotic compressibility data derived from static light-scattering data (eq 2) and the ratio D_{QELS}/D_{NMR} (eq 3): (A) $M = 4 \times 10^4$; (B) 7.4×10^4; (C) 1.45×10^6. Light scattering: (□), (●), and (×), D_{QELS}/D_{NMR}: (△), (▲), and (○). (b) Plots of osmotic compressibility data as a function of the excluded-volume parameter, X.[29] The broken line collects the experimental data from static LS and D_{QELS}/D_{NMR} while the whole line is given by eqs 4 and 5.

virial term may be estimated reliably in either way. This means that $f_{QELS} \simeq f_{NMR}$ in this concentration range.

It is also possible to estimate the inverse osmotic compressibility for a solution of interpenetrating coils of flexible chains employing the equation of Ohta and Oono,[29,30] derived using renormalization group theory.[28] The result is

$$[M/RT](\partial\pi/\partial C)_{T,P} = [1 + 1/8(9X - 2) + 2 \ln ([1 + X]/X)] \exp(1/4[1/X + [1 - 1/X^2] \ln (1 + X)]) \quad (4)$$

where X is a dimensionless parameter uniquely related to the second virial coefficient, A_2

$$X = [A_2 M_w C]/[9/16 - \ln (M_w/M_n)/8] \approx C/C^* \quad (5)$$

which is obtained by expanding eq 8 of ref 29 to first order in X.

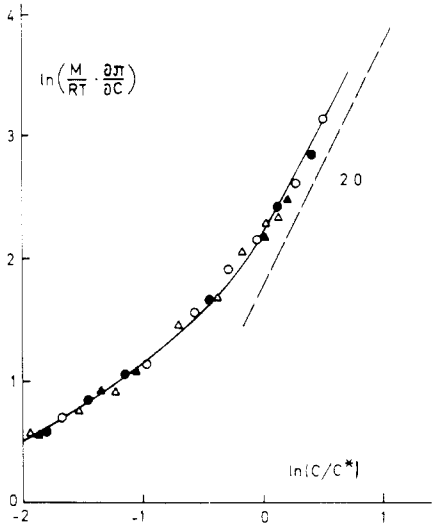

Figure 13. Determination of the concentration exponent for the reduced osmotic compressibility: $M = 4 \times 10^4$ (○); 7.4×10^4 (●); 1.45×10^5 (△); 5.94×10^5 (▲).

Figure 12b shows the combined experimental data from static LS and D_{QELS}/D_{NMR} (broken line) in terms of the excluded-volume term X compared with the theoretical expression of Ohta and Oono (full line) (eq 4). The agreement is gratifying, although at higher X values the divergence grows. A similar degree of divergence has also been demonstrated by Wiltzius et al.[33] and by Burchard[34] in flexible polymer/good solvent systems. The experimental data form a universal curve, approximately independent of solvent quality as long as $A_2 > 0$ and also independent of MW. Furthermore, polydispersity has little influence on the shape of the curve. When the simplified expression for X ($X = (16/9)A_2 C M_w$) is used, the values of $[M/RT](\partial\pi/\partial C)$ differ for all MW's by less than 5% from those obtained using eq 4.

Figure 13 is a logarithmic diagram of the reduced osmotic compressibility against C/C^*. When $C > C^*$, it is known that the exponent has the value 1.32 in a good solvent[47] and is approximately 2 in a Θ solvent. Our experimental data are in accord with the poor solvent value; a similar observation was made by Štěpánek et al.[35] for the polystyrene/cyclohexane Θ system. The static properties thus seem to be well expressed by current theory.

As regards the dynamic quantities, the theory for flexible chains is less well-developed. Figure 14a shows a comparison between the experimental data for a series of PEO fractions of different MW with predictions from Oono et al.[30]

$$D/D_0 = (1 + KC + ...) \quad (6)$$

where

$$KC = [\exp[\zeta/[8(1 + \zeta)]] - 3[\zeta/[8(1 + \zeta)]]/[1 - (1 + \zeta)^{-3/4}]]X \quad (7)$$

with $\zeta = 32z/3$ (see Freed et al.[28]). The z-parameter describes the excluded-volume effect and ranges between $z = \infty$ in good solvents to $z = 0$ in Θ solvents.

Figure 14a shows that the theoretical predictions are obeyed for low values of X. Thus, D/D_0 is independent of chain length. Furthermore, the concentration dependence is close (the coefficient K lies between 0.335 and 0.4 for all molecular weights) to that for a suspension of hard spheres,[31,32] as might be expected for coils in a poor (marginal) solvent. Thus we conclude that renormalization group theory gives a rather satisfactory description

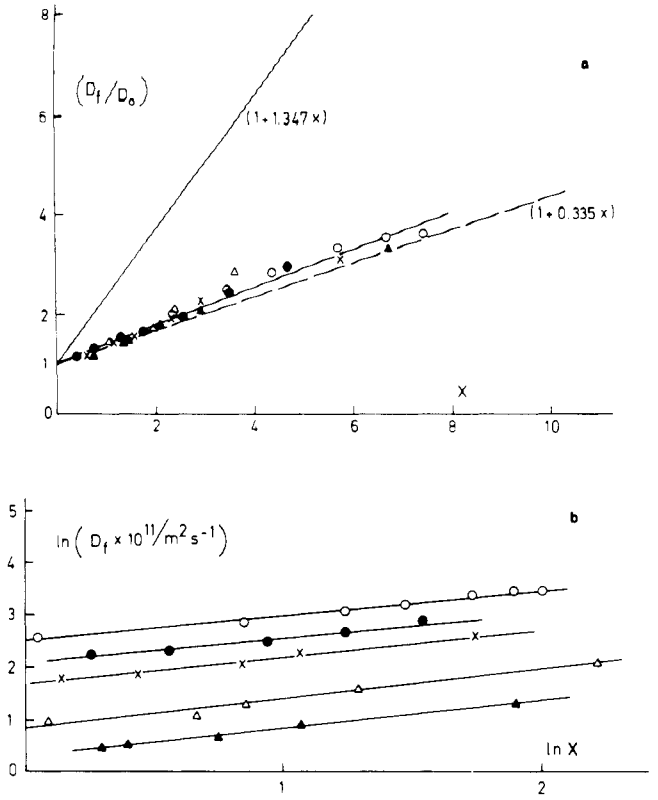

Figure 14. (a) Comparison of experimental data and those from renormalization group theory[29] for the dynamic quantity. (b) Scaling of the fast mode in terms of the excluded-volume parameter, X (eq 5). The exponent is 0.55 ($M = 4 \times 10^4$ (○); 7.4×10^4 (●); 1.45×10^5 (×); 5.94×10^5 (△); 1.2×10^6 (▲)).

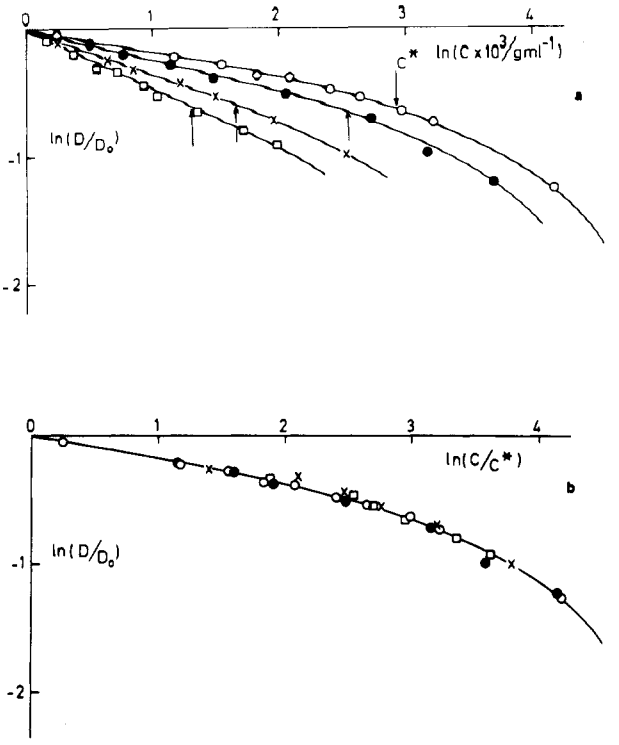

Figure 15. (a) Data for the diffusion of large SiO_2 spheres in PEO fraction ($M = 7.4 \times 10^4$ (○); 1.45×10^5 (●); 5.94×10^5 (×); 1.2×10^6 (□)). (b) Data in Figure 15a in terms of the normalized concentration (C/C^*).

of both the static and dynamic behavior of interpenetrating flexible chains in a poor solvent in the low X range.

Figure 14b shows the corresponding double-logarithmic diagram for testing the scaling hypothesis. The plots are close to linear and the average slope is 0.55. For flexible, linear chains, scaling arguments predict that in a good solvent the cooperative diffusion coefficient, D_c, is proportional to $X^{0.75}$ at $X \gg 1$. The situation in Θ solvents is less clear. We may note that recent measurements of the concentration dependence of the gel mode in Θ solvents at high values of the q vector on high molecular weight fractions of polystyrene gave an exponent of about 0.6.[36] This represents a large deviation from the exponent of unity anticipated in a Θ solvent for the hydrodynamic gel mode determined at low values of q. The latter exponent follows, owing to the compensation between monomer–monomer and monomer–solvent interactions. However, as pointed out by Deschamps and Léger,[37] real chains cannot cross and the chain motions may then be restricted by monomer–monomer contact points, which should lead to a lower concentration exponent.

Diffusion of Hard Spheres in PEO Solutions. Measurements were made of the diffusion of SiO_2 spheres (R_H = 1595 and 280 Å) in PEO solutions of various molecular weight and may be utilized to make comparisons with the diffusion of the molecular clusters since they have sizes of the same magnitude. Methanol is a poor solvent both for the stearic acid coated SiO_2 spheres and PEO. The decay time spectra were always bimodal, both peaks being q^2 dependent. The D values are self-diffusion coefficients obtained using trace amounts of SiO_2 spheres ($C = 5 \times 10^{-4}$ g mL^{-1}),which lay in the SiO_2 concentration region where sphere–sphere interactions are negligible (i.e., having zero concentration dependence of D_{sphere}). The measurements were made at an angle of 20°. The fast mode of low relative intensity is superimposable on the fast cooperative mode obtained with the PEO/methanol solutions considered above. The slow mode of dominant intensity must represent the SiO_2 spheres since at low concentrations it yields the correct hydrodynamic radius. The slow mode peak observed above in the PEO/methanol solutions is eclipsed by the SiO_2 peak (for the large spheres) as shown by comparison of their respective peak positions. Figure 15a shows log–log plots of the reduced translational diffusion coefficients of the large SiO_2 spheres. These fall off rapidly with increasing PEO concentration. When, however, the concentration is normalized using the overlap concentrations (C^*) for the different PEO fractions, a universal plot results. Similar behavior has been illustrated previously for SiO_2 spheres in other polymer systems[38] and is related to the scaling of the macroscopic viscosity with the reduced concentration, C/C^* (see Figure 6). The dependence of D/D_0 on molecular weight of the matrix may thus be expressed as $D/D_0 \sim M^{-0.58}$, which gives the dependence of C^* on M_{matrix}.

Figure 16 compares the reduced diffusion coefficient for stearic acid coated SiO_2 spheres of different sizes (R_H = 1595 and 280 Å) in a matrix of PEO ($M = 5.94 \times 10^5$) swollen in methanol. The reduced diffusion coefficient is strictly independent of sphere size. Theories such as that of Langevin and Rondelez,[39] based on scaling arguments for semidilute solutions, and that of Cukier[40,41] predict proportionality to the sphere radius while an earlier expression of Ogston et al.[42] gives a dependence on $R^{1/2}$. The present data agree, however, with the prediction of Altenberger et al.[43] who considered the motion of a Brownian particle through a rigid gel network generating hydrodynamic screening: the reduced mobility becomes independent of the particle radius. The results also agree with the experimental data of Phillies and coworkers[44,45] for latex particles diffusing in PEO solu-

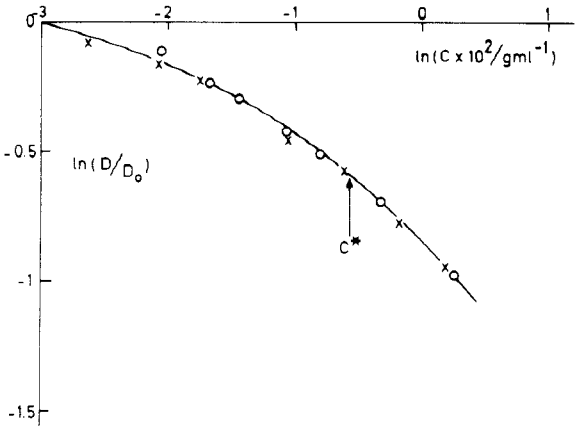

Figure 16. Comparison of SiO_2 diffusion for two sphere diameters, 1595 Å (○) and 280 Å (×), in PEO 5.94×10^5.

tions, where it was established that D/D_0 is almost independent of the probe particle radius.

We note here that the data for the SiO_2 spheres approximately coincide with those for the self-diffusion of the PEO chains determined by PFG-NMR. These data are included in the plot in Figure 5, illustrating the data in the form log (D/D_0) versus log (C/C^*), which is a universal curve for the NMR data. The clusters having approximately similar size to the large spheres (at a matrix polymer concentration of 1.3%) diffuse about 1 order of magnitude more slowly than the hard spheres. This suggests that a different mechanism is operative. One possibility is an apparent mobility associated with ordering into domains on a microscopic scale, these coexisting with disordered regions as postulated by Ito et al.[53,54] to describe phenomena in polymer/latex suspensions. We note also that "clustering" also occurs both in polymeric melts[55] as well as oligomeric systems[56] and may thus be a general phenomenon.

As discussed in connection with similar plots for data in the ternary polyisobutylene system, PIB1/PIB2/chloroform,[12] the coincidence of the hard-sphere data with those for the self-diffusion of the individual chains suggests that a reptational mechanism for the PEO self-diffusion is invalid.

Figure 17a shows the variation of the product $(D\eta)$ for the SiO_2 spheres in the PEO solutions. In general, the S–E equation is anticipated to be followed for large probes (of radius much greater than the matrix correlation length) in polymer solutions in which the entanglements relax comparatively rapidly and the polymer solution may be considered as a continuum. For all molecular weights the relaxation time of the large sphere is very much greater than the disentanglement time for the matrix chains (i.e., $\tau_{sphere} \gg T_R$, where $\tau_{sphere} \approx Dq^2_{\theta=20°}$) such that the polymer solution constitutes a viscous medium. T_R was evaluated as before using the expression given by de Gennes and Brochard.[46,47] However, for all molecular weights, $D\eta$ increases strongly with increasing C_{PEO} when the overlap concentration is exceeded. This trend has been noted before with, for example, these spheres diffusing in polyisobutylene (PIB) solutions except that with PEO the effect is much more pronounced. We note that the strong departure from Stokes–Einstein (S–E) behavior has been observed by Phillies[44,45] for latex spheres diffusing in aqueous polymer solutions. It is concluded that an increased in $D\eta$ with matrix concentration denoting departure from S–E behavior is a general phenomenon deriving from a coupling of the probe motions with those of the matrix polymer and may be expected to increase with increasing segment density of PEO and the strength of the interactions between particle and matrix chains.

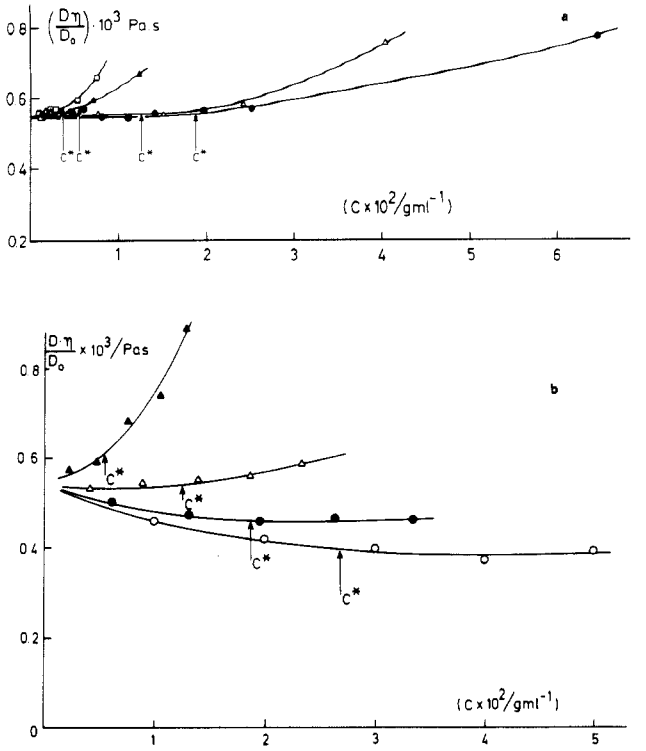

Figure 17. (a) Product $(D\eta)/D_0$ as a function of concentration for the large SiO_2 spheres (1595 Å) in PEO fractions (M = 7.4 × 10^4 (●); 1.45 × 10^5 (△); 5.94 × 10^5 (▲); 1.2 × 10^6 (□)). (b) Plot similar to that in Figure 17a but for the PEO self-diffusion coefficients determined by PFG-NMR (M = 4 × 10^4 (○); 7.4 × 10^4 (●) 1.48 × 10^5 (△), 5.94 × 10^5 (▲)).

Analogous plots to those in Figure 17a are shown in Figure 17b for the PFG-NMR self-diffusion data for the PEO fractions. $(D_{NMR}\eta)/D_0$ vs C_{PEO} for the various molecular weights indicate more complex behavior than for the self-diffusion of the SiO_2 spheres in PEO solutions. These plots show minor differences, which are not apparent in the log–log representation in Figure 5. Thus, the two lower MW fractions exhibit negative deviations from the concentration dependence expected from the S–E equation while the higher MWs show strong positive deviations as was noted for the SiO_2 spheres. This arises because the self-diffusion coefficient for linear chains decreases strongly with increasing concentration (see Figures 3 and 4), while on the other hand the bulk viscosity only starts to increase significantly above the entanglement concentration, C_E. Thus, these effects may be understood in terms of the interplay between inter-chain friction and the entanglement effects on viscosity. D_{NMR} initially decreases strongly with increasing coil concentration due to interchain friction, and only when the solutions have become entangled does the value of $D\eta$ start to increase.

Acknowledgment. This work was supported by the Swedish Natural Science Research Council (NFR) and the Swedish National Board for Technical Development (STU). P.Z. thanks the 1959 Ars fund for a stipendium.

References and Notes

(1) Brown, W.; Stilbs, P. *Polymer* **1982**, *23*, 1780.
(2) Brown, W., unpublished data.
(3) Polik, W. F.; Burchard, W. *Macromolecules* **1983**, *16*, 978.
(4) Brown, W. *Macromolecules* **1984**, *17*, 66.
(5) Kambe, U.; Honda, C. *Polymer* **1984**, *25* (Communication), 154.
(6) Brown, W. *Polymer* **1985**, *26*, 1647.

(7) Nyström, B.; Boileau, S.; Hemery, P.; Roots, J. *Eur. Polym. J.* **1981**, *17*, 249.
(8) Layec, Y.; Layec-Raphalen, M.-N. *J. Phys., Lett.* **1983**, *44*, L-121.
(9) Kim, H.; Chang, T.; Yohanan, J. M.; Wang, L.; Yu, H. *Macromolecules* **1986**, *19*, 2737.
(10) Wheeler, L. M.; Lodge, T. P.; Hanley, B.; Tirrell, M. *Macromolecules* **1987**, *20*, 1120.
(11) Nemoto, N.; Okada, S.; Inoue, T.; Kurata, M. *Macromolecules* **1988**, *21*, 1502; 1509.
(12) Brown, W.; Zhou, P. *Macromolecules* **1989**, *22*, 4031.
(13) von Meerwall, E. D.; Amis, E. J.; Ferry, J. D. *Macromolecules* **1985**, *18*, 260.
(14) Wesson, J. A.; Noh, I.; Kitano, T.; Yu, H. *Macromolecules* **1984**, *17*, 782.
(15) Jakes, J., submitted for publication in *Czech. J. Phys.*
(16) Provencher, S. W. *Makromol. Chem.* **1979**, *180*, 201.
(17) Geissler, E.; Hecht, A.-M. *J. Phys. Lett.* **1979**, *40*, L-173.
(18) Amis, E. J.; Han, C. C. *Polymer* **1982**, *23*, 1403.
(19) Amis, E. J.; Janmey, P. A.; Ferry, J. D.; Yu, H. *Macromolecules* **1983**, *16*, 441.
(20) Amis, E. J.; Han, C. C.; Matsushita, Y. *Polymer* **1984**, *25*, 650.
(21) Kolinski, A.; Skolnick, J.; Varis, R. *J. Chem. Phys.* **1987**, *86*, 1567, 7164, 7174.
(22) Brown, W.; Stilbs, P.; Johnsen, R. M. *J. Polym. Sci., Polym. Phys. Ed.* **1983**, *21*, 1029.
(23) Phillies, G. D. J. *J. Chem. Phys.* **1974**, *60*, 983; **1983**, *79*, 2325.
(24) Pusey, P. N.; Fijnaut, H. M.; Vrij, A. *J. Chem. Phys.* **1982**, *77*, 4270.
(25) Benmouna, M.; Benoit, H.; Duval, M.; Akcasu, Z. *Macromolecules* **1987**, *20*, 1107, 1112.
(26) Hanna, S.; Hess, W.; Klein, R. *Physica A (Amsterdam)* **1982**, *111A*, 181.
(27) Altenberger, A. R.; Tirrell, M. *J. Polym. Sci., Polym. Phys. Ed.* **1984**, *22*, 909.
(28) Feed, K. F. *J. Chem. Phys.* **1983**, *79*, 6357.
(29) Ohta, T.; Oono, Y. *Phys. Lett.* **1982**, *89A*, 460.
(30) Oono, Y.; Baldwin, P. R.; Ohta, T. *Phys. Rev. Lett.* **1984**, *53*, 2149.
(31) Batchelor, G. K. *J. Fluid Mech.* **1976**, *52*, 245.
(32) Hess, W.; Klein, R. *Physica A (Amsterdam)* **1976**, *85*, 509.
(33) Wiltzius, P.; Haller, H. R.; Cannell, D. S.; Schaefer, D. W. *Phys. Rev. Lett.* **1983**, *51*, 1183.
(34) Burchard, W., in press.
(35) Štěpánek, P.; Perzynsski, R.; Delsanti, M.; Adam, M. *Macromolecules* **1984**, *17*, 2340.
(36) Brown, W.; Johnsen, R. M.; Štěpánek, P.; Jakes, J. *Macromolecules* **1988**, *21*, 2859.
(37) Deschamps, H.; Léger, L. *Macromolecules* **1986**, *19*, 2760.
(38) Zhou, P.; Brown, W. *Macromolecules* **1989**, *22*, 890.
(39) Langevin, D.; Rondelez, F. *Polymer* **1978**, *14*, 875.
(40) Cukier, R. I. *J. Chem. Phys.* **1983**, *79*, 3911.
(41) Cukier, R. I. *Macromolecules* **1984**, *17*, 252.
(42) Ogston, A. G.; Preston, B. N.; Wells, J. D. *Proc. R. Soc. London, A* **1973**, *333*, 297.
(43) Altenberger, A. R.; Tirrell, M.; Dahler, J. S. *J. Chem. Phys.* **1986**, *84*, 5122.
(44) Phillies, G. D. J.; Ullmann, G. S.; Ullmann, K. *J. Chem. Phys.* **1985**, *82*, 5242.
(45) Ullmann, G. S.; Ullmann, K.; Lindner, R. M.; Phillies, G. D. J. *J. Phys. Chem.* **1985**, *89*, 692.
(46) Brochard, F.; de Gennes, P.-G. *Macromolecules* **1977**, *10*, 1157.
(47) de Gennes, P.-G. *Scaling Concepts in Polymer Physics*; Cornell University Press: London, 1979.
(48) Pike, E. R.; Pomeroy, W. R. M.; Vaughan, J. M. *J. Chem. Phys.* **1975**, *62*, 3188.
(49) von Meerwall, E. B. *J. Magn. Reson.* **1982**, *50*, 409.
(50) Eisele, M.; Burchard, W. *Macromolecules* **1984**, *17*, 1636.
(51) Sedlak, M.; Konak, C.; Štěpánek, P.; Jakes, J. *Polymer* **1987**, *28*, 873.
(52) Brown, W.; Stepanek, P. *Macromolecules* **1988**, *21*, 1791.
(53) Ito, K.; Okumura, H.; Yoshida, H.; Ueno, Y.; Ise, N. *Phys. Rev. B* **1988**, *38* (15), 10852.
(54) Ito, K.; Nakamura, H.; Yoshida, H.; Ise, N. *J. Am. Chem. Soc.* **1988**, *110*, 6955.
(55) Antonietti, M., personal communication.
(56) Meier, G., personal communication.

Registry No. PEO, 25322-68-3; CH_3OH, 67-56-1; SiO_2, 7631-86-9; stearic acid, 57-11-4.

Dipole Moments and Kerr Constants of Dibenzoates of Some Diols with Different Numbers of Methylene Units as Model Compounds for Polyesters

Francisco Mendicuti, Maria M. Rodrigo, Maria P. Tarazona, and E. Saiz*

Departamento de Quimica Fisica, Universidad de Alcala de Henares, 28871 Madrid, Spain.
Received February 1, 1989; Revised Manuscript Received June 1, 1989

ABSTRACT: Dipole moments and Kerr constants of dibenzoates of several diols have been measured at 25 °C. The general structure of these compounds can be represented as $C_6H_5COO(CH_2)_mOOCC_6H_5$ with m = 2–6. Dipole moments were obtained from determinations of dielectric constants and refractive indices in benzene solutions. The experimental results for the mean square dipole moments were $\langle\mu^2\rangle$ = 7.58, 6.71, 7.20, 7.43, and 7.74 D^2 for m = 2, 3, 4, 5, and 6 respectively. Kerr constants were evaluated from measurements of electric birefringence of solutions in cyclohexane (nearly isotropically polarizable solvent); experimental values obtained for m = 2, 3, 4, 5, and 6 were respectively ${}_mK$ = 29.1, 6.9, 11.6, 9.4, and 12.3 all in 10^{-25} m^5 V^{-2} mol^{-1}. Theoretical analysis was performed with standard method of the rotational isomeric states model. Comparison of theory with experiment indicates that $\langle\mu^2\rangle$ is almost insensitive to the conformational energies, particularly for $m > 3$; in fact, the free rotating model gives a reasonably good account for $\langle\mu^2\rangle$ for all of these molecules. Kerr constants are much more sensitive to the conformational energies. Good agreement between theoretical and experimental values of both dipole moments and Kerr constants of all these compounds is achieved by adjustment of the optical parameters and the position of the rotational isomers.

Introduction

Polyesters obtained by condensation of terephthalic acid (or any of its isomers) with different diols are an interesting kind of polymer whose repeating unit can be schematized as $C_6H_5COO(R)_mOOC$ where R represents a methylene (CH_2) group. Such repeating units combine a rigid residue coming from the acid with a flexible segment provided by the diol. The length of the flexible residue is controlled by the number m of R groups,

0024-9297/90/2223-1139$02.50/0